Λ_b^0-baryon production in pp collisions in the general-mass variable-flavour-number scheme, and comparison with CMS and LHCb data

G. Kramer[1] H. Spiesberger[2,3]

[1] II. Institut für Theoretische Physik, Universität Hamburg, Luruper Chaussee 149, D-22761 Hamburg, Germany
[2] Institut für Physik, Johannes-Gutenberg-Universität, Staudinger Weg 7, D-55099 Mainz, Germany,
[3] Centre for Theoretical and Mathematical Physics and Department of Physics, University of Cape Town, Rondebosch 7700, South Africa

Abstract: We calculate the next-to-leading-order cross section for the inclusive production of Λ_b baryons in pp collisions in the general-mass variable-flavor-number scheme. We use realistic evolved non-perturbative fragmentation functions obtained from fits to B-meson production in e^+e^- annihilation and compare our results for transverse-momentum and rapidity distributions with recent experimental data from the CMS and the LHCb collaborations at the CERN LHC. We find satisfactory agreement in general, with some indication for the need to modify the available fragmentation functions at larger values of the scale variable.

Keywords: heavy flavor production, perturbative QCD, Λ_b production

PACS: 12.38.Bx, 12.39.St, 13.85.Ni **DOI:** 10.1088/1674-1137/42/8/083102

1 Introduction

The study of the inclusive production of hadrons containing b quarks plays a particularly important role in testing quantum chromodynamics (QCD). The predictions in the framework of perturbative QCD are based on the factorization approach. Cross sections are calculated as a convolution of three terms: the parton distribution functions (PDF) encoding the parton content of the initial hadronic state, the partonic hard scattering cross sections computed as a perturbative series in powers of the strong coupling constant, and the fragmentation functions (FF), which describe the production yield and the momentum distribution for a given b hadron in a parton.

In the past, measurements of inclusive b-hadron production and the corresponding QCD calculations have been done mostly for B mesons, i.e., $B^{\pm}$, B^0, $\bar{B}^0$, B_s^0, and $\bar{B}_s^0$. Data for $p\bar{p}$ collisions at $\sqrt{S}=1.96$ TeV have been obtained at the FNAL Tevatron Collider [1, 2] and for pp collisions at $\sqrt{S}=7$, 8 and 13 TeV at the CERN Large Hadron Collider (LHC) by the CMS, ATLAS and LHCb collaborations [3–8]. The first measurement of the production cross section of a b baryon, Λ_b^0, has been performed by the CMS collaboration at the LHC [9] at $\sqrt{S}=7$ TeV using fully reconstructed $\Lambda_b^0 \to J/\psi\Lambda$ decays. CMS has measured the cross section as a function of the transverse momentum p_T and the rapidity y of the produced Λ_b^0 in the region $10 \leqslant p_T \leqslant 50$ GeV and in the central rapidity region $0 \leqslant |y| \leqslant 2$. The cross section ratio $\sigma(\bar{\Lambda}_b)/\sigma(\Lambda_b)$ has also been obtained in the same kinematic range. Later, the LHCb collaboration published similar measurements in the forward rapidity region $2.0 \leqslant y \leqslant 4.5$ in the p_T range $0 < p_T < 20$ GeV for $\sqrt{S}=7$ and 8 TeV [10]. Here, the measurement of Λ_b^0 production was based on the observation of the decay $\Lambda_b^0 \to J/\psi pK^-$.

Inclusive production of Λ_b baryons is of interest for several reasons. First, there is the question whether the perturbative approach to calculate b-quark production cross sections is applicable for the production of b baryons, as it is for the production of B mesons. Second, there is the more important question about details of the fragmentation of b quarks and other partons, for example of gluons, into b baryons. So far there exists almost no information on the Λ_b FF from earlier experiments. The new data from experiments at the LHC are therefore first of all valuable as they provide us with information needed to determine the Λ_b FF. The comparison of data for the production of Λ_b baryons with data for B-meson production could reveal unexpected differences between the Λ_b-baryon and B-meson fragmentation functions.

Third, there is the problem that incompatible results for the b hadron production fractions have been found in different measurements. The relative production rates of b hadrons are described by the fragmentation fractions

Received 29 March 2018, Published online 20 June 2018

$f_{\rm u}$, $f_{\rm d}$, $f_{\rm s}$, $f_{\rm c}$, and $f_{\rm baryon}$ for the probability that a b quark fragments into a $B_{\rm q}$ meson (q = u,d,s,c) or a b baryon. It is assumed that $f_{\rm u} = f_{\rm d}$, and $f_{\rm baryon} = f_{\Lambda_{\rm b}}$ is obtained from $\Lambda_{\rm b}$ production. According to the most recent analysis of the Heavy Flavor Averaging Group (HFAG [11]) one finds $f_{\rm u} = f_{\rm d} = 0.412 \pm 0.008$, $f_{\rm s} = 0.088 \pm 0.013$, and $f_{\rm baryon} = 0.089 \pm 0.012$ when determined from LEP data for $Z \to b\bar{b}$ decays only, but Tevatron data lead to $f_{\rm u} = f_{\rm d} = 0.340 \pm 0.021$, $f_{\rm s} = 0.101 \pm 0.015$, and $f_{\rm baryon} = 0.218 \pm 0.047$. Only for $f_{\rm s}$ do these values agree well, while for the $\Lambda_{\rm b}$ baryon fragmentation fraction there is a discrepancy of more than a factor of two. These results are clearly not compatible with the assumption that the b-hadronization fractions are universal. Further evidence for this non-universality comes from LHCb data where a strong dependence of $f_{\Lambda_{\rm b}}$ on the transverse momentum was observed [12, 13]. If the difference in data for $f_{\Lambda_{\rm b}}/f_{\rm d}$ obtained from LEP or from $p\bar{p}$ (pp) colliders is confirmed, one should conclude that the production mechanism for $\Lambda_{\rm b}$ (and alike for other b hadrons) is affected by the presence of strongly interacting particles in the initial state, e.g., by the proton remnants emitted in the extreme forward direction.

In our calculation of $\Lambda_{\rm b}$-baryon production we shall use the FF for $b \to B$ as obtained in Ref. [14] from LEP data [15–18]. For the light-quark fragmentation fractions we shall assume in the following the value $f_{\rm u} = f_{\rm d} = 0.401$ [19], which is very close to the value in our previous work [14].

The first evidence that $f_{\Lambda_{\rm b}}/f_{\rm d}$ is different in hadron collisions compared with values determined in e^+e^- annihilation was found at the CDF experiment [20]. It was suggested in the publication by CDF that there may be a strong dependence on the kinematic properties of the produced b quark. The b jets in Z decays at LEP have $p_{\rm T} \simeq 40$ GeV, while the average $p_{\rm T}$ of the measurement at CDF is 15 GeV. Measurements at the LHCb experiment probe an even lower $p_{\rm T}$ range. A strong scale dependence is, however, not consistent with theoretical predictions. For example, in Ref. [14] we could demonstrate that the $b \to B$ fragmentation fraction (denoted $B(\mu)$ in Ref. [14] and evaluated as the integral over the $b \to B$ FF) depends only very little on the scale μ varying in the range between 4.5 and 91.2 GeV. Unfortunately there are no data from CDF for the $p_{\rm T}$ spectrum and we have to restrict a detailed comparison of kinematic properties of B-meson and $\Lambda_{\rm b}$-hadron production to data from the LHC. We note that a comparison with data also requires input for the branching ratios of $\Lambda_{\rm b}$-hadrons to observed final states, which often are known only with large uncertainties.

The purpose of this work is to study the cross section for inclusive production of $\Lambda_{\rm b}$ baryons in the framework of the general-mass variable-flavour-number scheme (GM-VFNS) [21, 22]. This framework has provided a good description for b-meson production in $p\bar{p}$ collisions at $\sqrt{S} = 1.96$ TeV at the FNAL Tevatron Collider [14] and in pp collisions at $\sqrt{S} = 7$ TeV at the CERN LHC by the CMS, ATLAS and LHCb collaborations [3–7, 23, 24].

The GM-VFNS is essentially the conventional next-to-leading order (NLO) QCD parton-model approach supplemented with finite-mass effects, intended to improve the description at small and medium transverse momenta $p_{\rm T}$. The original GM-VFNS formulation [21, 22, 25] was, however, not suitable for the calculation of the cross section at very small transverse momenta $p_{\rm T}$. This was caused by the specific choice of the scale parameter $\mu_{\rm I}$ for the initial-state factorization as $\mu_{\rm I} = \sqrt{m_{\rm b}^2 + p_{\rm T}^2}$, where $m_{\rm b}$ is the mass of the b quark. As a consequence of this choice, only at $p_{\rm T} = 0$ does the scale parameter approach $\mu_{\rm I} = m_{\rm b}$, where the b-quark parton distribution function (PDF) vanishes (in almost all available PDF parametrizations). Therefore the transition to the fixed-flavour number scheme (FFNS), which is the appropriate scheme for calculating $d\sigma/dp_{\rm T}$ at small $p_{\rm T} < m_{\rm b}$, is not reached for non-zero $p_{\rm T} > 0$. The original GM-VFNS prescription was therefore modified later. In Ref. [24, 26] we have shown that a smooth transition to the FFNS at finite $p_{\rm T} > 0$ can be obtained by choosing the factorization scale appropriately. With the choice $\mu_{\rm I} = 0.5\sqrt{m_{\rm b}^2 + p_{\rm T}^2}$ instead of $\mu_{\rm I} = \sqrt{m_{\rm b}^2 + p_{\rm T}^2}$, a reasonably good description of the experimental data for B-meson production down to $p_{\rm T} = 0$ could be achieved for the CDF data [1] in $p\bar{p}$ collision at the Tevatron and for the LHCb data [27] in pp collisions at the LHC at $\sqrt{S} = 7$ TeV. Since the recent measurements of the inclusive $\Lambda_{\rm b}$ production cross sections at the LHCb extend down to $p_{\rm T} = 0$ [10] we will apply the GM-VFNS with this modified scale choice. For the CMS data which are at higher $p_{\rm T}$ well above the b-quark threshold, we keep the original setting of scales.

The plan of the paper is as follows. In Section 2 we introduce our strategy and describe our choice of the proton PDFs and the FFs for the transition $b \to \Lambda_{\rm b}^0$. In Section 3 we collect our results for inclusive $\Lambda_{\rm b}$ production at $\sqrt{S} = 7$ TeV and compare with the CMS data published in Ref. [9]. A similar comparison is then performed in Section 4 for LHCb data [10] at $\sqrt{S} = 7$ and 8 TeV in the forward rapidity range $2.0 < y < 4.5$. Here we study also the cross section ratios of the 7 and 8 TeV data and ratios of the inclusive production cross sections for $\Lambda_{\rm b}$ and B^0 mesons. Our conclusions are presented in Section 5.

2 Setup and input

The theoretical foundation of the GM-VFNS framework as well as technical details of its implementation have been presented previously in Refs. [21, 22]. Here we

describe only the input required for the numerical calculations discussed below. For the proton PDFs we use the set CTEQ14 [28] as implemented in the LHAPDF library [29]. We take the b-quark pole mass to be $m_{\rm b}$=4.5 GeV and evaluate the strong coupling $\alpha_{\rm s}^{(n_{\rm f})}(\mu_{\rm R})$ at NLO with $\Lambda_{\overline{MS}}^{(4)}=328$ MeV for $n_{\rm f}=4$. This corresponds to $\Lambda_{\overline{MS}}^{(5)}=226$ MeV above the 5-flavor threshold of the renormalization scale chosen at $\mu_{\rm R}=m_{\rm b}$.

For simplicity, in the following sections we take the initial- and final-state factorization scales, entering the PDFs and FFs, respectively, to have the same value, denoted by $\mu_{\rm F}$. We choose $\mu_{\rm F}$ and the renormalization scale $\mu_{\rm R}$, at which $\alpha_{\rm s}$ is evaluated, to be $\mu_{\rm F}=\xi_{\rm F}\mu_0$ and $\mu_{\rm R}=\xi_{\rm R}\mu_0$, where μ_0 will be specified in the next two sections, when we compare our results to the CMS and LHCb data. In the calculation of cross sections to be compared with the CMS data we shall vary the parameters $\xi_{\rm F}$ and $\xi_{\rm R}$ about their default values $\xi_{\rm F}$=$\xi_{\rm R}$=1 up and down by factors of 2 (with the restriction $1/2<\xi_{\rm R}/\xi_{\rm F}<2$). For comparisons with the LHCb data we restrict ourselves to variations of the renormalization scale factor $\xi_{\rm R}$.

We employ the non-perturbative B-meson FFs determined in Ref. [14]. These FFs were obtained by fitting experimental data for inclusive production in e^+e^- annihilation taken by the ALEPH [15] and OPAL [16] collaborations at CERN LEP1 and by the SLD collaboration [17, 18] at SLAC SLC. Since these data were all taken on the Z-boson resonance, $\alpha_{\rm s}^{(n_{\rm f})}(\mu_{\rm R})$ was evaluated with $n_{\rm f}=5$ and the renormalization and factorization scales were fixed at $\mu_{\rm F}$=$\mu_{\rm R}$=$m_{\rm Z}$ in Ref. [14]. The starting scale μ_0 of the b$\to$B FF was chosen to be μ_0=$m_{\rm b}$ in accordance with Ref. [28]. Below $\mu_{\rm F}$=μ_0 the light-quark and gluon FFs for q,g$\to$B (including the charm quark, i.e., q=u,d,s,c) were assumed to vanish. A simple power ansatz has yielded the best fit to the experimental data.

One should notice that the B-meson FFs of Ref. [14] do not distinguish between different b-hadron states. In fact, the OPAL [16] and SLD [17, 18] data include all b hadrons, i.e., the mesons $B^{\pm}$, $B^0/\bar{B}^0$ and $B_s^0/\bar{B}_s^0$ as well as b-baryons, such as Λ_b^0, while in the ALEPH [15] analysis, only final states with identified $B^{\pm}$ and $B^0/\bar{B}^0$ mesons were taken into account[1)]. Despite the differences in the experimental analyses of ALEPH, OPAL and SLD it was assumed in Ref. [14] that the data can be described by one common FF. They were normalized to provide cross sections for the B^+ or B^0 mesons. They can also be used to calculate b-quark production by removing the fragmentation fraction for the b$\to B^+$ transition, which was assumed as $f_{\rm d}=f_{\rm u}=0.397$ in Ref. [14]. We assume that $\Lambda_{\rm b}$ production is also described by the same FF and that only the normalization has to be adjusted, i.e., the same FF multiplied by $f_{\Lambda_{\rm b}}/f_{\rm d}$ can be used to obtain the FF for b$\to\Lambda_{\rm b}^0$.

3 Comparison with CMS data

CMS has measured the cross section for $\Lambda_{\rm b}^0$ production at $\sqrt{S}=7$ TeV in the central rapidity region $-2.0<y<2.0$ and for $p_{\rm T}$ in the range $10<p_{\rm T}<50$ GeV [9]. The data are given for the differential cross sections $\mathrm{d}\sigma/\mathrm{d}p_{\rm T}$ and $\mathrm{d}\sigma/\mathrm{d}|y|$ multiplied with the branching ratio for the decay $\Lambda_{\rm b}^0\to \mathrm{J}/\psi\Lambda$. We calculate $\mathrm{d}\sigma/\mathrm{d}p_{\rm T}$ integrated over $|y|$ and $\mathrm{d}\sigma/\mathrm{d}y$ integrated over the considered $p_{\rm T}$ range with the same binning as chosen by CMS.

The default renormalization and factorization scale is chosen as $\mu_0=\sqrt{m_{\rm b}^2+p_{\rm T}^2}$ and an estimate of theoretical uncertainties is obtained by varying $\xi_{\rm R}$ and $\xi_{\rm F}$ as described above. We multiply the calculated cross sections by $Br(\Lambda_{\rm b}^0\to \mathrm{J}/\psi\Lambda)f_{\Lambda_{\rm b}}/f_{\rm d}=(1.45\pm0.20)\times10^{-4}$. This is obtained from $f_{\rm d}$=0.401 and the latest PDG value for $f_{\Lambda_{\rm b}}Br(\Lambda_{\rm b}^0\to \mathrm{J}/\psi\Lambda)=(5.8\pm0.8)\times10^{-5}$ [31].

Our results are compared with the experimental data in Figs. 1 and 2. The errors of the experimental data points are obtained from Ref. [9] by adding in quadrature the statistical and systematic errors quoted there. The error of the branching ratio $Br(\Lambda_{\rm b}^0\to \mathrm{J}/\psi\Lambda)$ does not contribute. The left side of Fig. 1 shows $\mathrm{d}\sigma/\mathrm{d}p_{\rm T}$ times branching ratio integrated over the rapidity $|y|<2.0$, and the left side of Fig. 2 shows $\mathrm{d}\sigma/\mathrm{d}y$ integrated over $p_{\rm T}$ in the measured range $10<p_{\rm T}<50$ GeV. We find agreement between theory and data for the three lowest $p_{\rm T}$ bins within the theory error band, but for the three upper $p_{\rm T}$-bins the experimental values of $\mathrm{d}\sigma/\mathrm{d}p_{\rm T}$ lie outside the error band from variations of the scale parameters. The prediction of $\mathrm{d}\sigma/\mathrm{d}p_{\rm T}$ for the largest $p_{\rm T}$ bin is larger by a factor of approximately 2 as compared to the experimental point. This is seen more clearly in the right-hand panel of Fig. 1, where we have plotted the ratio of the measured cross section with respect to the theory prediction. The full-line histogram is obtained from data normalized to the prediction with the default scale, the dashed-line histograms are found when normalizing data to the minimal scale choice (upper dashed-line histogram) or maximal scale choice (lower dashed-line histogram). For readability the experimental errors are shown only for the default scale. The comparison in Fig. 1 may be taken as an indication that the FF for b$\to\Lambda_{\rm b}$ behaves differently compared to the FF for b$\to$B meson. For example, the stronger decrease of the data with increasing $p_{\rm T}$ could be obtained if the maximum of the $\Lambda_{\rm b}$ FF was shifted to smaller z as compared to the B-meson FF. A similar conclusion was suggested in Ref. [9], based on a comparison of data for $\Lambda_{\rm b}^0$, B^+, and B^0 production with predictions from POWHEG [32, 33]

1) A more recent study of b-hadron fragmentation by the DELPHI collaboration [30] is using b-tagged final states which also combine all b-hadrons. These data agree with the earlier ALEPH, OPAL and SLD measurements within their experimental uncertainties.

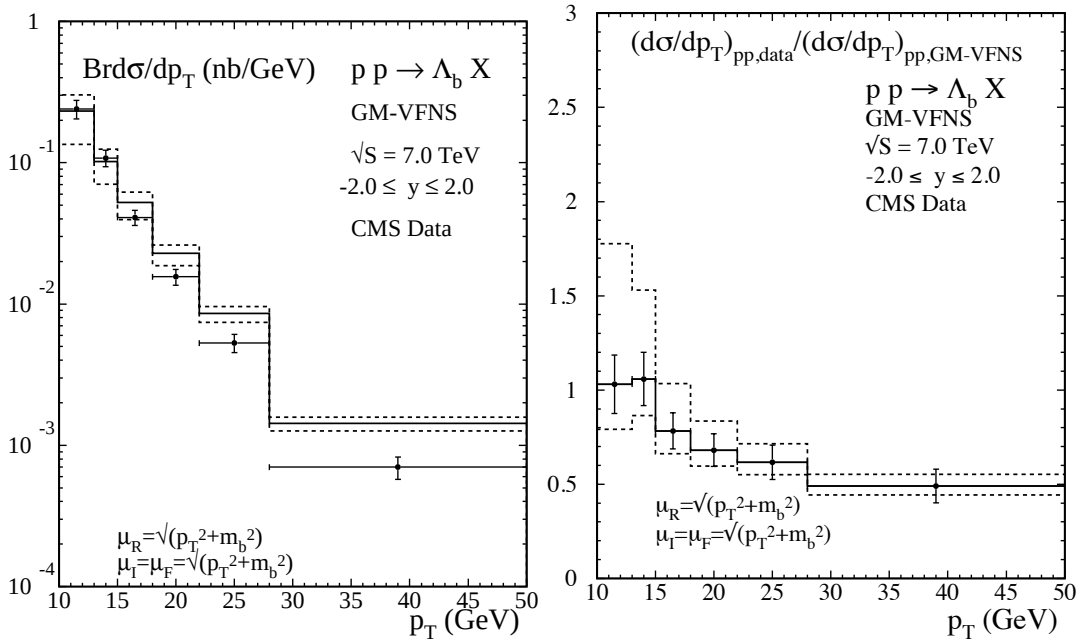

Fig. 1. Left panel: Differential cross section $\mathrm{d}\sigma/\mathrm{d}p_{\mathrm{T}}$ times branching ratio $Br(\Lambda_{\mathrm{b}}^0 \to \mathrm{J}/\psi\Lambda)$ of prompt inclusive Λ_{b}^0-baryon production in the GM-VFNS for $\sqrt{S}=7.0$ TeV pp collisions with $|y|<2.0$ compared to CMS data [9]. The upper and lower dashed histograms are calculated with μ_{R} and $\mu_{\mathrm{I}}=\mu_{\mathrm{F}}$ changed independently by factors of 1/2 and 2 with the restriction $1/2<\mu_{\mathrm{R}}/\mu_{\mathrm{F}}<2$. Right panel: Ratios of data over theory. For the central, full-line histogram the CMS data are normalized to the calculated cross sections for the default scale (full line in the left panel). The upper/lower dashed-line histograms are the ratios of data normalized to the predictions with scales that lead to the minimal/maximal cross sections (dashed lines in the left panel). Experimental uncertainties are shown by error bars only for the central curve.

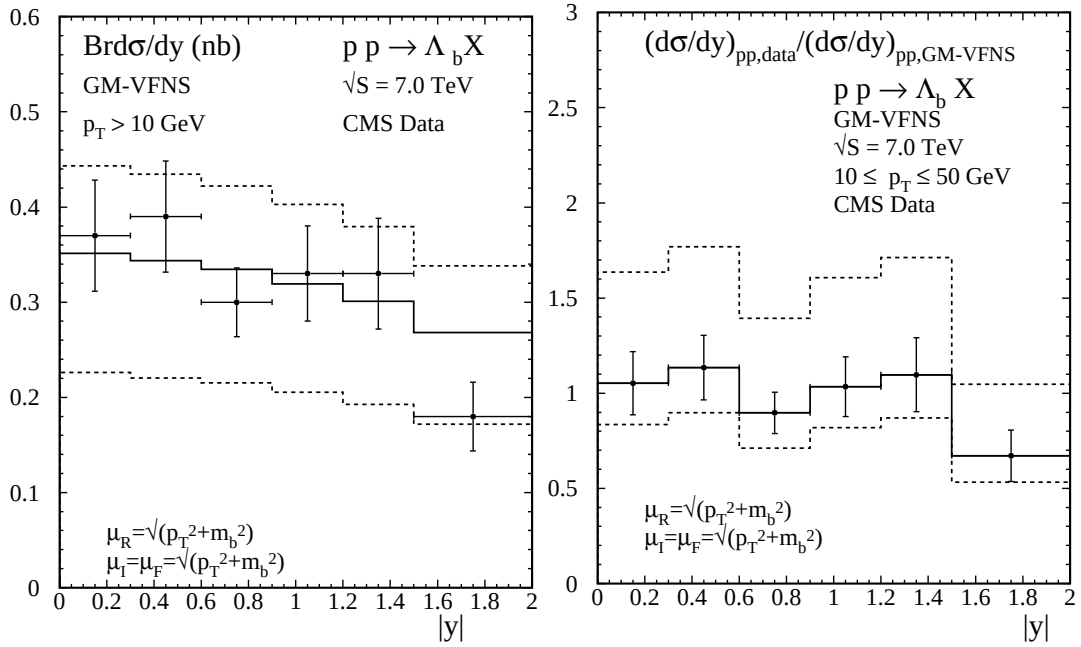

Fig. 2. Differential cross section $\mathrm{d}\sigma/\mathrm{d}y$ times branching ratio for prompt inclusive Λ_{b}^0-baryon production in the GM-VFNS for $\sqrt{S}=7.0$ TeV pp collisions for $10\leqslant p_{\mathrm{T}}\leqslant 50$ GeV compared with CMS data [9]. The upper and lower dashed histograms are calculated with μ_{R} and $\mu_{\mathrm{I}}=\mu_{\mathrm{F}}$ varied independently by factors of 1/2 and 2. The ratios of data over theory in the right panel are calculated as described above (see caption of Fig. 1).

and PYTHIA [34]. The predictions from PYTHIA agree with data at low $p_{\rm T}$, but over-estimate data at large $p_{\rm T}$, very similar to our results. In contrast, POWHEG is in better agreement with data for the large-$p_{\rm T}$ bins, but below data at low $p_{\rm T}$. Since low $p_{\rm T}$ dominate for all values of y, the POWHEG prediction for $\mathrm{d}\sigma/\mathrm{d}y$ is below data by almost a factor of 2 in the whole y range.

The prediction for $\mathrm{d}\sigma/\mathrm{d}y$ as a function of $|y|$ between 0 and 2 is shown in Fig. 2, left panel, compared to the CMS data. It agrees quite well with the experimental data even for the default scale choice, except for the bin $1.5<|y|<2.0$. This is, of course, consistent with the comparison of the $p_{\rm T}$-differential cross section. The ratio of data and the calculated cross sections times branching ratio are shown in the right panel of Fig. 2.

4 Comparison with LHCb data

The LHCb collaboration has measured $\Lambda_{\rm b}^0$ production in pp collisions at $\sqrt{S}=7$ TeV in 2011 and $\sqrt{S}=8$ TeV in 2012 [10]. The data extend to small transverse momenta, $0<p_{\rm T}<20$ GeV, in the forward-rapidity range, $2.0<y<4.5$. The $p_{\rm T}$-differential cross sections are presented in five rapidity bins between $y=2.0$ and 4.5 and in 10 (12) $p_{\rm T}$ bins between 0 and 20 GeV for the 7 TeV (8 TeV) measurements, respectively. Since the shape of the distributions as a function of $p_{\rm T}$ is very similar for all values of y and differ only by their normalization, we find it sufficient to compare our predictions with data for $\mathrm{d}\sigma/\mathrm{d}p_{\rm T}$ integrated over the full y range, $2.0<y<4.5$. We determine the corresponding values by summing the original data given in Ref. [10] over the five y bins. The uncertainties are obtained correspondingly by adding the statistical and systematic errors of the bins linearly and then combining statistical and systematic errors in quadrature to obtain a total uncertainty.

The $\Lambda_{\rm b}^0$ baryons were identified in the decay $\Lambda_{\rm b}^0 \to \mathrm{J/\psi pK^-}$ and results are therefore given as cross sections times branching ratio of this decay. This branching ratio is deduced in Ref. [10] from the ratio of the cross sections for $\Lambda_{\rm b}^0$ and $\bar{\rm B}^0$ production at 7 and 8 TeV. Unfortunately the cross section data in Ref. [10] are given for the sum of $\rm B^0$+$\bar{\rm B}^0$ production and not just for $\bar{\rm B}^0$ production. Therefore the ratio shown in Fig. 6 of Ref. [10] should be multiplied by two to determine $R_{\Lambda_{\rm b}^0/\bar{\rm B}^0}$ and we find for the branching ratio $Br(\Lambda_{\rm b}^0 \to \mathrm{J/\psi pK^-}) = (6.34\pm1.24)\times10^{-4}$ where the errors given in Ref. [10] are summed in quadrature. The analysis of Ref. [10] leading to this value is based on input for $f_{\Lambda_{\rm b}}/f_{\rm d}$ which was taken from Fig. 3 (right panel) of Ref. [13]. At $p_{\rm T}$ = 5 GeV one has $f_{\Lambda_{\rm b}}/f_{\rm d}=0.50$. This is combined in $Br(\Lambda_{\rm b}^0\to\mathrm{J/\psi pK^-})f_{\Lambda_{\rm b}}/f_{\rm d}=(3.17\pm0.62)\times10^{-4}$. We shall use this value for the branching ratio times $f_{\Lambda_{\rm b}}/f_{\rm d}$ in our calculations to obtain the cross section for $\Lambda_{\rm b}^0$ production.

In the low $p_{\rm T}$ range relevant for the LHCb data we have to choose the factorization scale following our previous work [24, 26]. Only with $\mu_{\rm I}=\mu_{\rm F}=0.5\sqrt{m_{\rm b}^2+p_{\rm T}^2}$ (instead of $\mu_{\rm I}=\mu_{\rm F}=\sqrt{m_{\rm b}^2+p_{\rm T}^2}$ as in the previous section) we find a smooth transition of the GM-VFNS prescription to the FFNS. The default renormalization scale is fixed at $\mu_{\rm R}=\sqrt{p_{\rm T}^2+m_{\rm b}^2}$ and variations by factors of 1/2 and 2 are studied to obtain an estimate of the theoretical uncertainty.

Our results are shown in Fig. 3 for $\sqrt{S}=7$ TeV and in Fig. 4 for $\sqrt{S}=8$ TeV. Full-line histograms show the results for the default scales $\mu_{\rm F}=0.5\sqrt{m_{\rm b}^2+p_{\rm T}^2}$, $\mu_{\rm R}=\sqrt{m_{\rm b}^2+p_{\rm T}^2}$; the dashed-line histograms represent the estimate of theoretical uncertainties due to the variation of the renormalization scale. In the right-hand panels of these figures we display the ratios of data over theory. As above we show the experimental error bars only for the central prediction, but the maximal and minimal values of the ratios have errors of the same magnitude as the central prediction. Taking account of these experimental uncertainties, as well as of uncertainties due to scale variations, we find in general a good agreement between data and theory, both for $\sqrt{S}=7$ TeV and for $\sqrt{S}=8$ TeV. The exceptions are the two data points at the lowest $p_{\rm T}$ values and maybe the one at largest $p_{\rm T}$.

We should remember that the FFs have been determined from $\rm e^+e^-$ data which are dominated by B-meson production. It is therefore instructive to verify that they can also be used to describe B-meson production in pp collisions. For this purpose we show plots for the sum of $\rm B^0$+$\bar{\rm B}^0$ production at 7 and 8 TeV in Figs. 5 and 6, respectively. As before, we show both the differential cross sections $\mathrm{d}\sigma/\mathrm{d}p_{\rm T}$ times branching ratio (left panels) and ratios of data over theory (right panels) and compare with LHCb data [10]. The agreement of the data with our predictions looks very similar to the case of $\Lambda_{\rm b}^0$ production, except for the data point at the largest $p_{\rm T}$: for $\rm B^0$+$\bar{\rm B}^0$ there is good agreement within errors, whereas for $\Lambda_{\rm b}^0$ production the corresponding data point was outside the error bands. This could indicate that the $\Lambda_{\rm b}^0$-production cross section decreases somewhat faster with increasing $p_{\rm T}$ than the $\rm B^0$+$\bar{\rm B}^0$-production cross section.

Differences between B-meson and $\Lambda_{\rm b}$-baryon production are more clearly exhibited in Fig. 7. Here we show the ratios of the $p_{\rm T}$ distributions for inclusive $\Lambda_{\rm b}^0$ over $\rm B^0$ production as a function of $p_{\rm T}$. The differential cross sections $\mathrm{d}\sigma/\mathrm{d}p_{\rm T}$ are multiplied with the respective branching fractions to obtain the results shown in this figure for $\sqrt{S}=7$ TeV (left panel) and $\sqrt{S}=8$ TeV (right panel). The horizontal line at the ratio $=0.248$ represents the theoretical prediction. It is independent of $p_{\rm T}$ since we have assumed that the same FF is responsible for b-meson and for b-hadron production, i.e., only

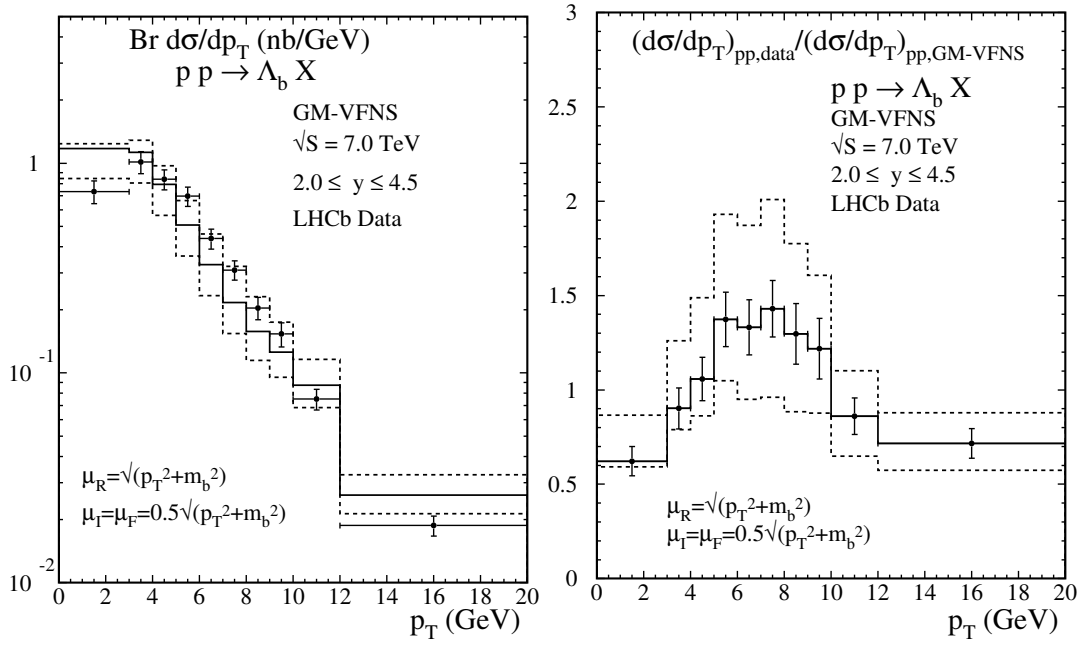

Fig. 3. Differential cross section $\mathrm{d}\sigma/\mathrm{d}p_{\mathrm{T}}$ times branching ratio for prompt inclusive Λ_{b}^0-baryon production in the GM-VFNS for $\sqrt{S}=7.0$ TeV pp collisions with $2.0\leqslant y\leqslant 4.5$ compared to LHCb data [10]. The upper and lower dashed histograms are calculated with μ_{R} changed by factors 1/2 and 2. The ratios of data over theory in the right panel are calculated as described above (see caption of Fig. 1).

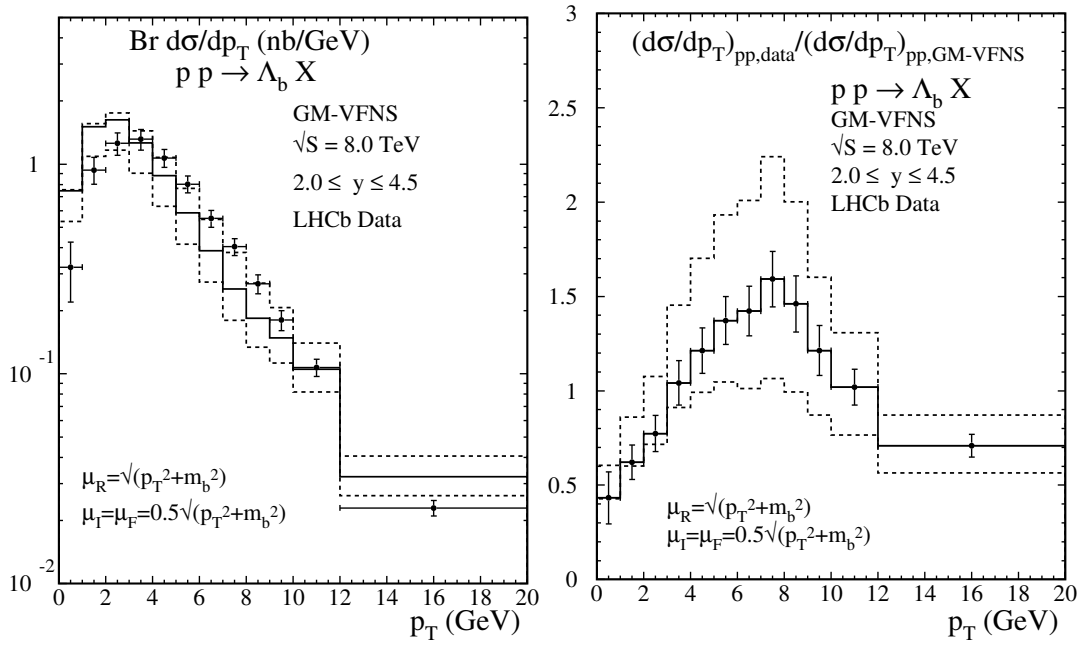

Fig. 4. Differential cross section $\mathrm{d}\sigma/\mathrm{d}p_{\mathrm{T}}$ times branching ratio for prompt inclusive Λ_{b}^0-baryon production in the GM-VFNS for $\sqrt{S}=8.0$ TeV pp collisions with $2.0\leqslant y\leqslant 4.5$ compared to LHCb data [10]. The upper and lower dashed histograms are calculated with μ_{R} changed by factors 1/2 and 2. The ratios of data over theory in the right panel are calculated as described above (see caption of Fig. 1).

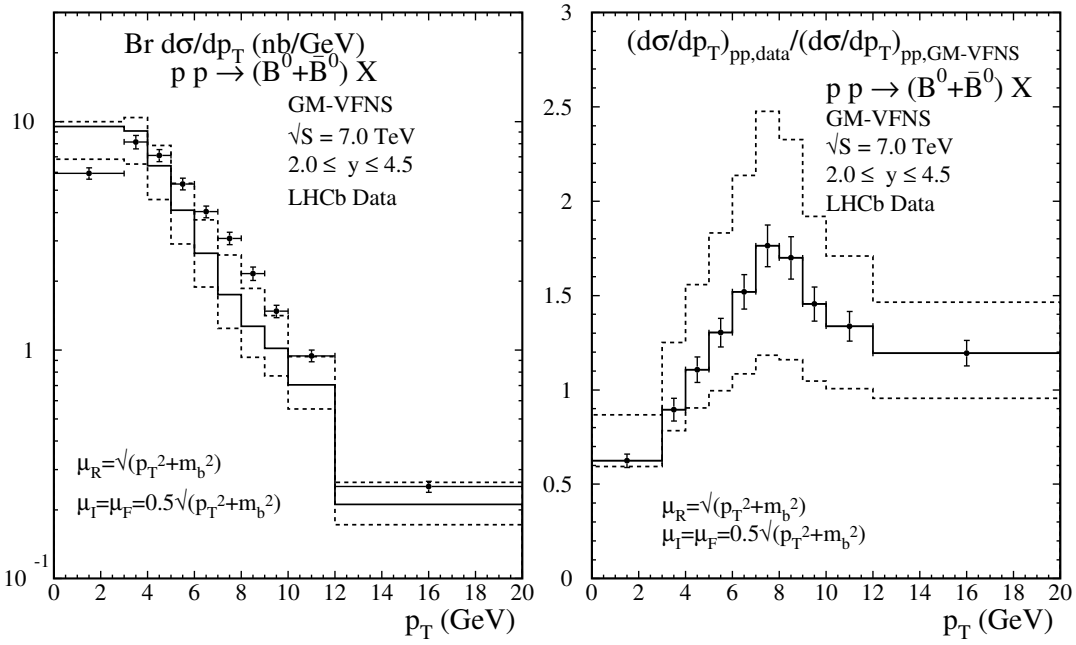

Fig. 5. Differential cross section $\mathrm{d}\sigma/\mathrm{d}p_{\mathrm{T}}$ times branching ratio of prompt inclusive $(\mathrm{B}^0+\bar{\mathrm{B}}^0)$-meson production in the GM-VFNS for $\sqrt{S}$=7.0 TeV pp collisions with $2.0\leqslant y\leqslant 4.5$ compared to LHCb data [10]. The upper and lower dashed histograms are calculated with μ_{R} changed by factors 1/2 and 2. The ratios of data over theory in the right panel are calculated as described above (see caption of Fig. 1).

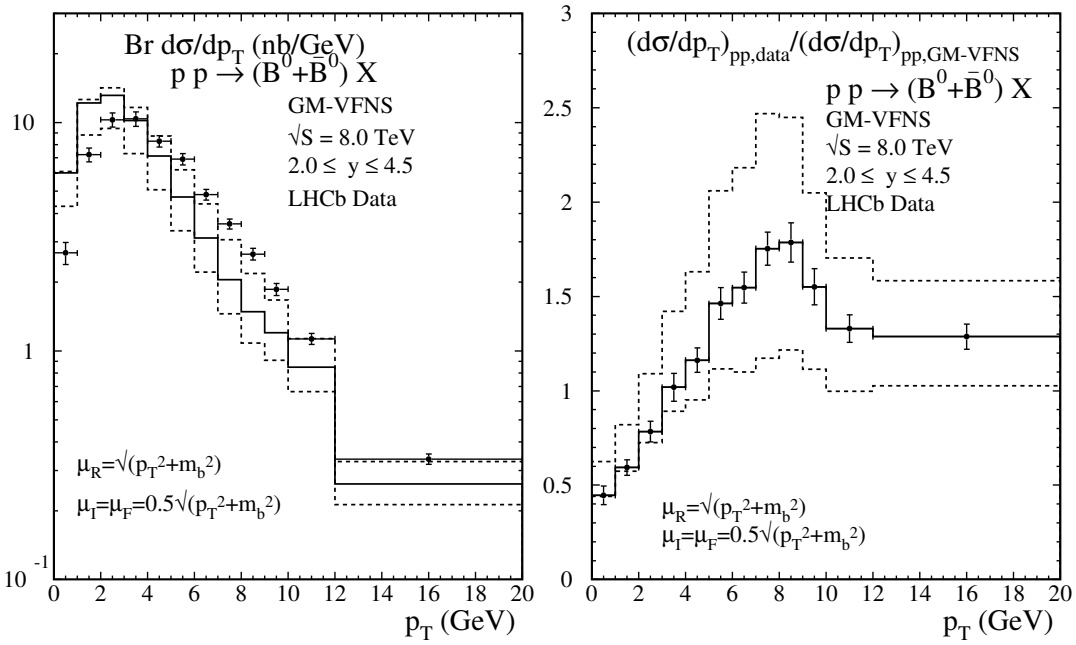

Fig. 6. Differential cross section $\mathrm{d}\sigma/\mathrm{d}p_{\mathrm{T}}$ times branching ratio of prompt inclusive $(\mathrm{B}^0+\bar{\mathrm{B}}^0)$-meson production in the GM-VFNS for $\sqrt{S}$=8.0 TeV pp collisions with $2.0\leqslant y\leqslant 4.5$ compared to LHCb data [10]. The upper and lower dashed histograms are calculated with μ_{R} changed by factors 1/2 and 2. The ratios of data over theory in the right panel are calculated as described above (see caption of Fig. 1).

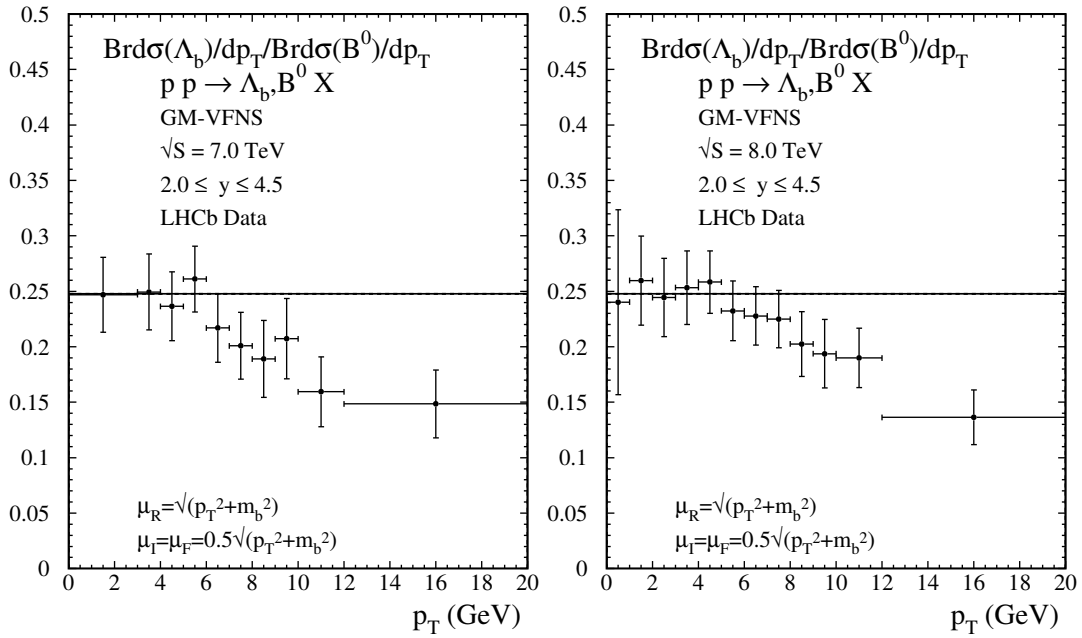

Fig. 7. Ratios of production cross sections $\mathrm{d}\sigma/\mathrm{d}p_{\mathrm{T}}$ times branching fractions for prompt inclusive Λ_{b}^{0} over B^{0} production as a function of p_{T} for $\sqrt{S}$=7.0 TeV (left) and $\sqrt{S}$=8.0 TeV (right).

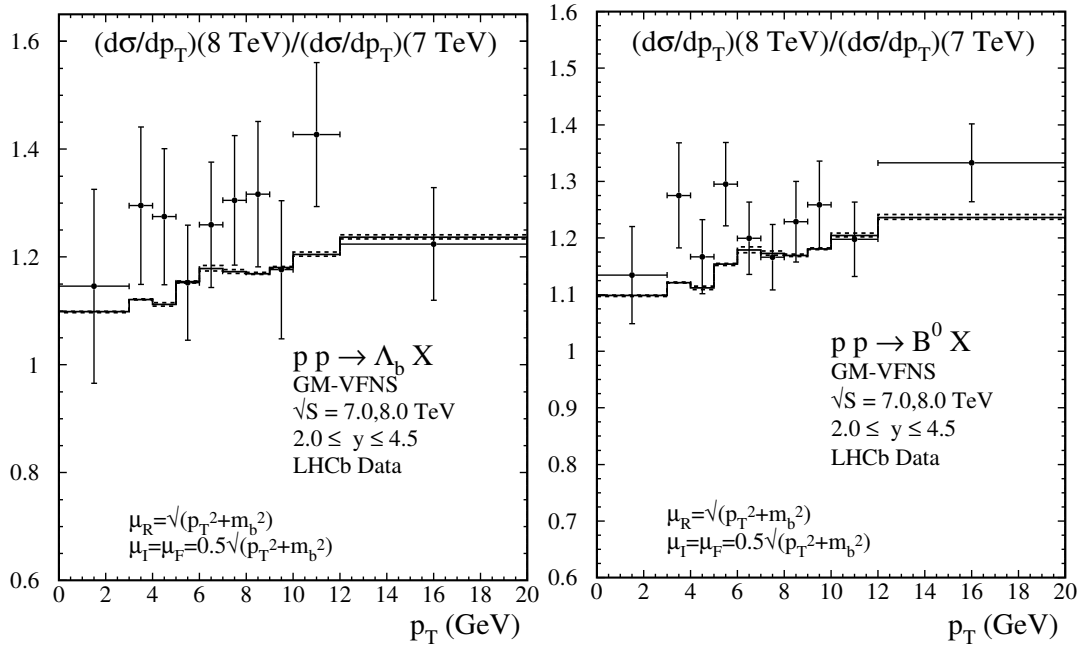

Fig. 8. Cross section ratios $\mathrm{d}\sigma/\mathrm{d}p_{\mathrm{T}}$ for prompt Λ_{b}^{0} (left) and B^{0} (right) production at $\sqrt{S}$=8.0 TeV over $\sqrt{S}$=7.0 TeV compared with LHCb data [10].

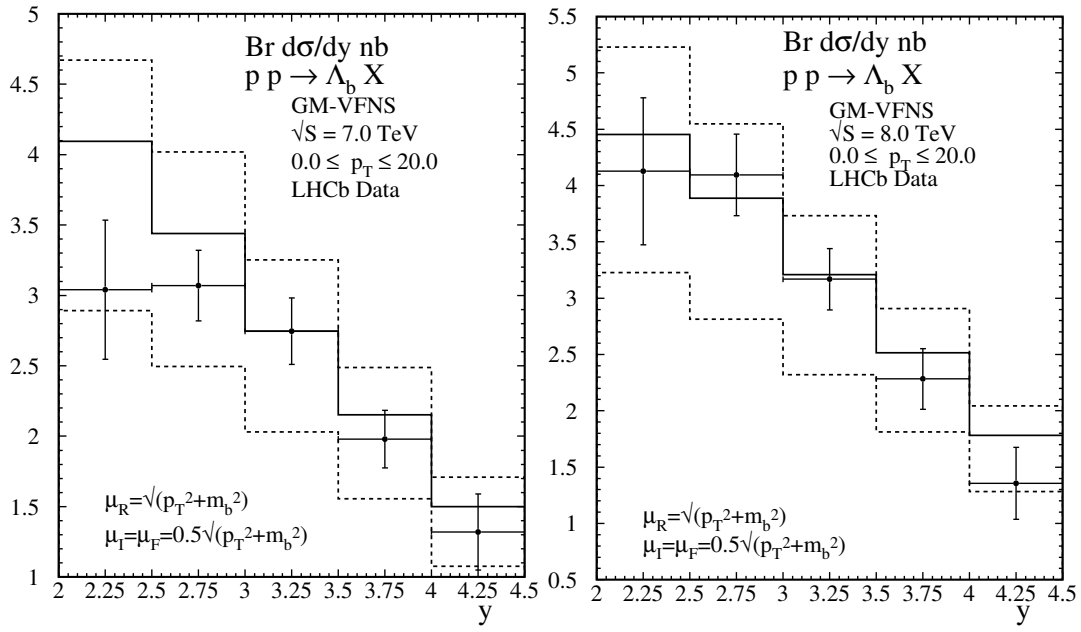

Fig. 9. Cross sections dσ/dy times branching ratio for prompt inclusive Λ_b^0 production at $\sqrt{S}$=7.0 TeV (left) and $\sqrt{s}$=8.0 (right) compared to LHCb data [10].

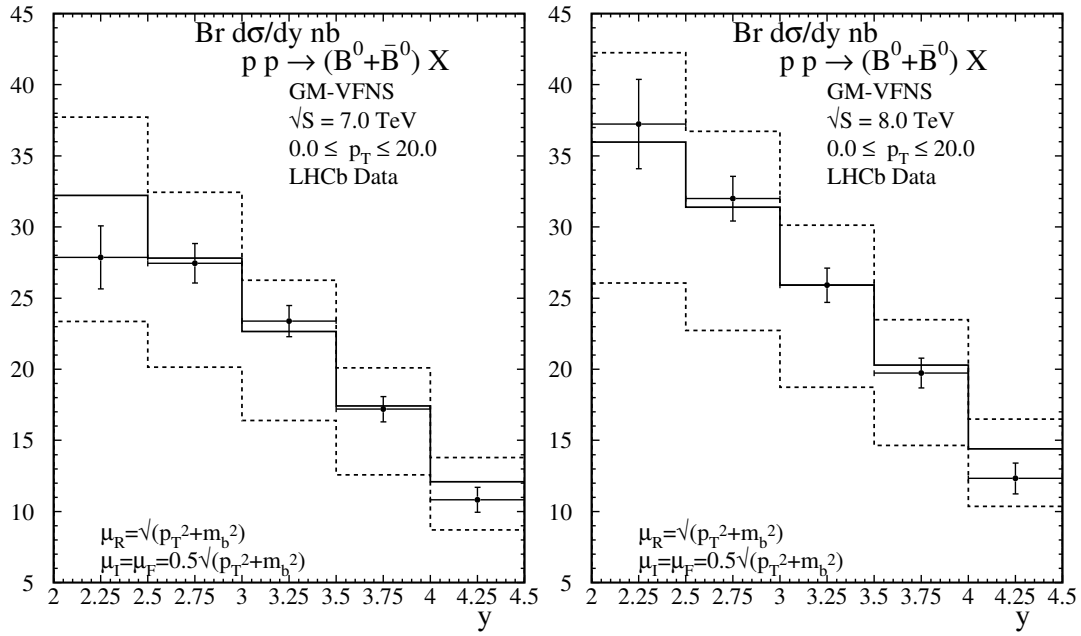

Fig. 10. Cross sections dσ/dy times branching ratio for prompt inclusive $B^0+\bar{B}^0$ production at $\sqrt{S}$=7.0 TeV (left) and $\sqrt{s}$=8.0 (right) compared to LHCb data [10].

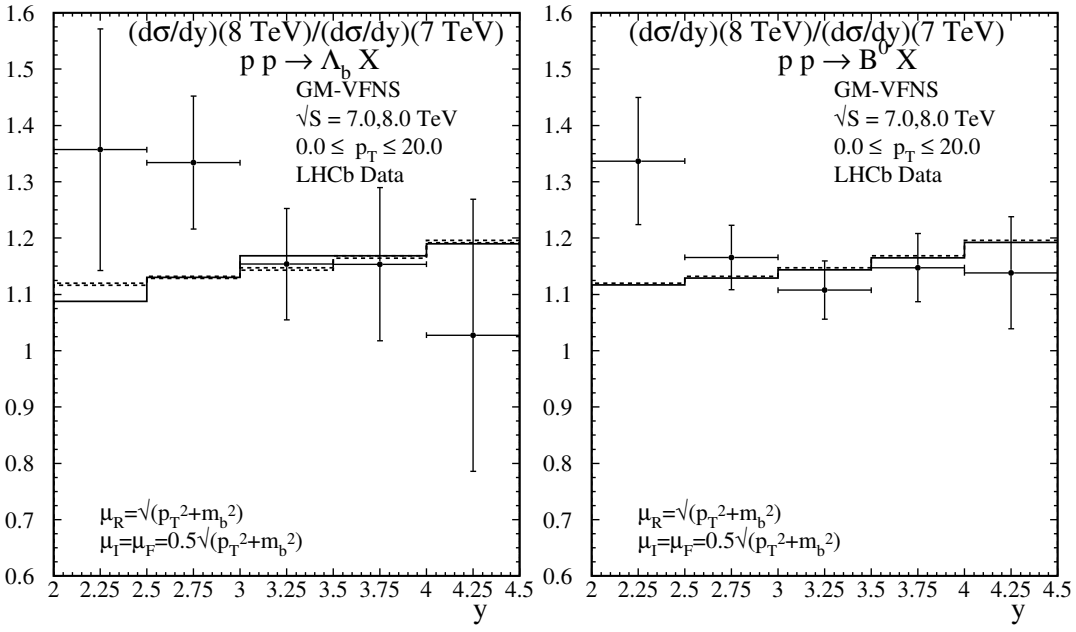

Fig. 11. Ratio of production cross sections $\mathrm{d}\sigma/\mathrm{d}y$ for $\sqrt{s}$=8.0 TeV over $\sqrt{s}$=7.0 TeV for Λ_b^0 (left) and B^0 production (right) compared to LHCB data [10].

the corresponding branching fraction times the ratio of the fragmentation fractions f_{Λ_b}/f_d has to be calculated. The experimental values for this ratio decrease with increasing p_T, fall below the theoretical prediction above $p_T = 7$ GeV (8 GeV) for $\sqrt{S} = 7$ TeV (8 TeV), respectively, and reach the value $\simeq 0.15$ in the bin with largest p_T.

We emphasize that this ratio is particularly well suited to compare the FFs for $b \to \Lambda_b^0$ and $b \to B^0$ fragmentation since it is not affected by theoretical uncertainties due to scale variations. The errors shown in Fig. 7 are purely experimental and we have added the uncertainties of the corresponding cross sections in quadrature. A full experimental analysis as performed in Ref. [10] can take into account correlations, which leads to a partial cancellation of uncertainties in the ratio. Results[1)] have been shown in Fig. 6 of Ref. [10] with a similar conclusion, but significantly smaller errors.

It may also be instructive to study the $\sqrt{S}$ dependence of the production cross sections. In Fig. 8 we show the ratios of cross sections at $\sqrt{S}$=8 TeV over those at $\sqrt{S}$=7 TeV for both Λ_b^0 (left panel) and B^0 production (right panel). Our calculation is compared with LHCb data [10]. For both final states the ratios vary between 1.1 and 1.2 as a function of p_T. For B^0 production the agreement with data is somewhat better than for Λ_b^0 production, but the uncertainties and statistical fluctuations are still too large to draw a definitive conclusion.

Finally we present results for the rapidity distributions. The cross sections $\mathrm{d}\sigma/\mathrm{d}y$ times the respective branching ratios for Λ_b^0 and B^0 production as a function of y for five bins in the range $2.0<y<4.5$ are shown in Fig. 9. The left and right panels are for $\sqrt{S}=7$ and 8 TeV, respectively. Our predictions are compared with LHCb data [10]. We have obtained the corresponding cross section values from Tables 3 – 6 of Ref. [10], summing the data for the double-differential cross sections $\mathrm{d}^2\sigma/\mathrm{d}p_T\mathrm{d}y$ given there over the p_T bins in the range $0<p_T<20$ GeV. For each p_T bin, statistical and systematic errors are added linearly first, then the errors are combined quadratically to obtain the total uncertainties shown in Fig. 9. We find quite satisfactory agreement between predictions and data. Similar results for $B^0+\bar{B}^0$ production are shown in Fig. 10, again for $\sqrt{S}=7$ (left panel) and 8 TeV (right panel) and also compared with experimental data from Ref. [10]. The agreement between predictions and data is similarly good as for the case of Λ_b^0 production.

Ratios of $\mathrm{d}\sigma/\mathrm{d}y$ for $\sqrt{S}=7$ over 8 TeV for Λ_b^0 and B^0 production have been shown in Ref. [10] as well. We present corresponding theoretical predictions in Fig. 11. Again, our calculation of the errors does not take into account correlations, and the experimental uncertainties found in Ref. [10] are somewhat smaller than in our plots. Apart from this difference we find results which are quite similar to the ratios calculated with the FONNL

1) Note, however, that we have defined the Λ_b^0/B^0 ratio as normalized to the cross section for B^0 production, not for $B^0+\bar{B}^0$ production as in Ref. [10].

approach [35, 36], also given in Ref. [10].

5 Conclusions

We have performed a detailed study of next-to-leading-order predictions for inclusive b-hadron production in pp collisions within the general-mass variable-flavor-number scheme. Our predictions are based on the assumption that B-meson and Λ_b^0-baryon production can be described by a common fragmentation function and that only constant branching fractions have to be chosen appropriately. The comparison with data for Λ_b^0-baryon production from the CMS and the LHCb collaborations at the CERN LHC shows agreement in the overall picture. However, at larger transverse momenta, the data from both experiments, which cover different rapidities, fall below the predictions. In particular the ratio of Λ_b^0-baryon over B-meson production exhibits indications that the fragmentation functions need to be modified at larger values of the scale variable. We expect that future data with reduced experimental uncertainties will help to clarify the situation.

We thank Michael Schmelling for helpful correspondence about the LHCb publication [10].

References

1 D. Acosta et al (CDF Collaboration), Phys. Rev. D, **71**: 032001 (2005) [hep-ex/0412071]
2 A. Abulencia et al (CDF Collaboration), Phys. Rev. D, **75**: 012010 (2007) [hep-ex/0612015]
3 V. Khachatryan et al (CMS Collaboration), Phys. Rev. Lett., **106**: 112001 (2011) [arXiv: 1101.0131 [hep-ex]]
4 S. Chatrchyan et al (CMS Collaboration), Phys. Rev. Lett., **106**: 252001 (2011) [arXiv: 1104.2892 [hep-ex]]
5 S. Chatrchyan et al (CMS Collaboration), Phys. Rev. D, **84**: 052008 (2011) [arXiv: 1106.4048 [hep-ex]]
6 G. Aad et al (ATLAS Collaboration), JHEP, **1310**: 042 (2013) [arXiv: 1307.0126 [hep-ex]]
7 R. Aaij et al (LHCb Collaboration), JHEP, **1204**: 093 (2012) [arXiv: 1202.4812 [hep-ex]]
8 V. Khachatryan et al (CMS Collaboration), Phys. Lett. B, **771**: 435 (2017) [arXiv: 1609.00873 [hep-ex]]
9 S. Chatrchyan et al (CMS Collaboration), Phys. Lett. B, **714**: 136 (2012) [arXiv: 1205.0594 [hep-ex]]
10 R. Aaij et al (LHCb Collaboration), Chin. Phys. C, **40**: 011001 (2016) [arXiv: 1509.00292 [hep-ex]]
11 Y. Amhis et al (HFLAV Collaboration), Eur. Phys. J. C, **77**: 895 (2017) [arXiv: 1612.07233 [hep-ex]]
12 R. Aaij et al (LHCb Collaboration), Phys. Rev. D, **85**: 032008 (2012) [arXiv: 1111.2357 [hep-ex]]
13 R. Aaij et al (LHCb Collaboration), JHEP, **1408**: 143 (2014) [arXiv: 1405.6842 [hep-ex]]
14 B. A. Kniehl, G. Kramer, I. Schienbein, and H. Spiesberger, Phys. Rev. D, **77**: 014011 (2008) [arXiv: 0705.4392 [hep-ph]]
15 A. Heister et al (ALEPH Collaboration), Phys. Lett. B, **512**: 30 (2001) [hep-ex/0106051]
16 G. Abbiendi et al (OPAL Collaboration), Eur. Phys. J. C, **29**: 463 (2003) [hep-ex/0210031]
17 K. Abe et al (SLD Collaboration), Phys. Rev. Lett., **84**: 4300 (2000) [hep-ex/9912058]
18 K. Abe et al (SLD Collaboration), Phys. Rev. D, **65**: 092006 (2002); Phys. Rev. D, **66**: 079905 (2002) [hep-ex/0202031]
19 J. Beringer et al (Particle Data Group), Phys. Rev. D, **86**: 010001 (2012)
20 T. Aaltonen et al (CDF Collaboration), Phys. Rev. D, **77**: 072003 (2008) [arXiv: 0801.4375 [hep-ex]]
21 B. A. Kniehl, G. Kramer, I. Schienbein, and H. Spiesberger, Phys. Rev. D, **71**: 014018 (2005) [hep-ph/0410289]
22 B. A. Kniehl, G. Kramer, I. Schienbein, and H. Spiesberger, Eur. Phys. J. C, **41**: 199 (2005) [hep-ph/0502194]
23 B. A. Kniehl, G. Kramer, I. Schienbein, and H. Spiesberger, Phys. Rev. D, **84**: 094026 (2011) [arXiv: 1109.2472 [hep-ph]]
24 B. A. Kniehl, G. Kramer, I. Schienbein, and H. Spiesberger, Eur. Phys. J. C, **75**: 140 (2015) [arXiv: 1502.01001 [hep-ph]]
25 B. A. Kniehl, G. Kramer, I. Schienbein, and H. Spiesberger, Eur. Phys. J. C, **72**: 2082 (2012) [arXiv: 1202.0439 [hep-ph]]
26 G. Kramer and H. Spiesberger, Phys. Lett. B, **753**: 542 (2016) [arXiv: 1509.07154 [hep-ph]]
27 R. Aaij et al (LHCb Collaboration), JHEP, **1308**: 117 (2013) [arXiv: 1306.3663 [hep-ex]]
28 S. Dulat et al, Phys. Rev. D, **93**: 033006 (2016) [arXiv: 1506.07443 [hep-ph]]
29 A. Buckley, J. Ferrando, S. Lloyd, K. Nordström, B. Page, M. Rüfenacht, M. Schönherr, and G. Watt, Eur. Phys. J. C, **75**: 132 (2015) [arXiv: 1412.7420 [hep-ph]] http://projects.hepforge.org/lhapdf/pdfsets
30 J. Abdallah et al (DELPHI Collaboration), Eur. Phys. J. C, **71**: 1557 (2011) [arXiv: 1102.4748 [hep-ex]]
31 C. Patrignani et al (Particle Data Group), Chin. Phys. C, **40**: 100001 (2016)
32 S. Alioli, P. Nason, C. Oleari, and E. Re, JHEP, **1006**: 043 (2010) [arXiv: 1002.2581 [hep-ph]]
33 S. Frixione, P. Nason, and G. Ridolfi, JHEP, **0709**: 126 (2007) [arXiv: 0707.3088 [hep-ph]]
34 T. Sjöstrand, S. Mrenna, and P. Z. Skands, JHEP, **0605**: 026 (2006) [hep-ph/0603175]
35 M. Cacciari, M. Greco, and P. Nason, JHEP, **9805**: 007 (1998) [hep-ph/9803400]
36 M. Cacciari, S. Frixione, N. Houdeau, M. L. Mangano, P. Nason, and G. Ridolfi, JHEP, **1210**: 137 (2012) [arXiv: 1205.6344 [hep-ph]]